Polish J. Chem., **76**, 1271–1285 (2002)

FT-IR Studies of CH…B Interactions in Fluoroform Containing Cryosolutions*

by S.M. Melikova[1], K.S. Rutkowski[1], P. Rodziewicz[2] and A. Koll[2]**

[1]*Institute of Physics, St. Petersburg University,*
1 Ulianovskaja st., 198504 St. Petersburg, Peterhof, Russia
[2]*Faculty of Chemistry, University of Wrocław, 14 F. Joliot-Curie, 50-383 Wrocław, Poland*

(Received September 25th, 2001; revised manuscript March 14th, 2002)

A transition from a blue shifted frequency of the ν(CH) vibrations of CF_3H to a conventional red frequency shift, accompanied by unusually varying integrated intensity of the corresponding ν_1 band, have been studied in CF_3H/B systems, where B = Ar, N_2, CO, CO_2, $O(CD_3)_2$, NH_3, and $N(CD_3)_3$. DFT/B3LYP and *ab initio* MP2 calculations, utilizing the 6-311++G(3df,3pd) basis set, predict a weakly H-bond-like linear F_3CH…B complex formation in the series studied and reproduce experimentally observed variations of spectroscopic parameters. The results obtained are treated in the framework of induced dipole moment, taking into account opposite directions of the CH bond dipole moment and the dipole moment of the whole molecule. In the range of overtone and combination bands of fluoroform, new weak bands have been detected. They were attributed to simultaneous excitations of vibrations of interacting CF_3H and B (= CO, CO_2) molecular pairs.

Key words: fluoroform, CH...B interaction, hydrogen bond, vibrational spectra, blue shift

A red shift of the fundamental stretching frequency -ν(A–H) and increased integrated intensity of the respective A–H band are characteristic features of a conventional H-bond of the A–H…B type [1–3]. Here, A and B are electronegative elements or groups with a region of high electron density. Usually, B possesses one or more lone electron pairs. It may also belong to unsaturated or aromatic compounds with π-electron system. A larger separation of the positive and negative charges, caused by an elongation of the A–H bond, results in a larger dipole moment and makes interaction more attractive in these conventional H bonded complexes. A relative decrease in the first overtone 2ν(AH) band intensity is often considered as an additional important characteristics of H-bonding [4,5]. Analogous, but markedly smaller effects of red frequency shift and intensity growth are often observed for fundamental stretching bands of molecules embedded in liquid solvents [6]. In this case, the ordinary internal field effect is taken into account by the Lorentz's field correction for the measured values of frequency and integrated intensity [6,7]. Usually, the internal field correction of the intensity growth does not exceed ~ 10 ÷15%. If bulk's nature interactions cause noticeable variation of molecular electric parameters (first at all the

* Presented at the 1st Russian-Ukrainian-Polish Conference on Molecular Interactions in Gdańsk, June 2001, (Poland).

** Corresponding author e-mail: melikova@molsp.phys.spbu.ru; fax: (7-812) 4287240.

dipole moment function), the Onsager reaction field model [8] can be used to treat, at least qualitatively, the solvent effect on the integrated intensity of molecular stretching band. Evaluations, based on the reaction field model, are often less successful and convincing for the frequency shift effect. It is due to competition between attractive and repulsion forces, defining specifics of intermolecular interactions.

Systems marked as A–H...B, where A = Hal, O, and N are the most frequently and best studied [1–5]. Compounds containing atom S or P as the element A might form somewhat weaker H-bonded complexes, characterized by a conventional red frequency shift [9]. Although carbon is markedly less electronegative, now it is recognized that a CH group can also form an H bond [10–17], with B = Hal, N, and O atoms [10–14] or B = π-electron containing compounds [14–17]. Recent theoretical studies suggest more complicated features in the case of some CH…B (*e.g.* when B = O or π electron system) complex formation, as compared with the effects of intensity growth and red frequency shift, generally accepted for conventional H-bonds [10,18–22]. The first experimental observations of the opposite effects, *i.e.* considerable blue shift of frequency accompanied by decrease of integrated intensity were reported for the CH-stretching vibration band (ν_1) of fluoroform dissolved in liquefied Ar and N_2 [23,24]. Unusual variation of frequency shift and integrated intensity of ν_1 band were found in the series of $F_3CH...B$ systems (B = CD_3F, $(CD_3)_2O$, $(C_2D_5)_2O$, $(CD_3)_3N$ and $(C_2D_5)_3N$) [25]. Experiments with triformylmethane in chloroform also seem to suggest a blue frequency shift [26]. Qualitatively analogous unusual behavior has been reported for mixed systems of chloroform and some proton acceptor containing compounds [27]. At last, recent experiments on $B^-…H_3Hal$ (B^- = Cl^-, I^-, Hal = Br, I) seem to confirm theoretically predicted very large blue shifts in these anionic complexes [22].

In the present study, new results on the unconventional change of the spectroscopic parameters, caused by the specific type interactions, are reported. Theoretical treatment of the observed effects based on DFT and *ab initio* MO calculations is also given. IR spectra of fluoroform dissolved in liquefied Ar, N_2, CO and CO_2 have been measured in the range of about 1000 up to 9000 cm^{-1}. The features of higher order transitions up to the $3\nu_1$ overtone, together with the ν_1 band, are studied. $F_3CH…NH_3$ and $F_3CH…N(CD_3)_3$ complexes are also considered for comparison of spectroscopic features of weakly bond systems and noticeably more stable heterodimers, both containing fluoroform as a CH proton donor.

EXPERIMENTAL AND COMPUTATIONAL METHODS

FT-IR spectra have been studied from about 1000 up to 9000 cm^{-1} with resolution of 0.5÷1.0 cm^{-1}. They were recorded using a Nicolet (Nexus) spectrometer. Two cryogenic cells with an optical path length of 1.0 cm and 8.5 cm and with BaF_2 windows were used. They have been built into a homemade cryostat cooled by liquid nitrogen. The spectroscopic measurements lies within the limits T ~ 100÷120 K (Ar, N_2, and CO) and T ~ 230÷250 K (CO_2). Temperature of the sample was measured with an accuracy of ~3 K. The concentration of fluoroform in liquid Ar, N_2, CO and CO_2 solutions was varied between 10^{16}÷10^{21} molec/cm^3. Due to less solubility, the concentration of fluoroform did not exceed 10^{19}

molec/cm^3 and about 10^{20} molec/cm^3 in the case of Ar, N_2 and CO respectively. The technique and experimental procedures were analogous to those used in studies of overtone and combination bands in ClH…CO weakly bond system [28]. The absolute integrated intensity of the bands studied has been evaluated with an accuracy of about 25%. Inaccuracy of an intensity ratio does not exceed 10% for the majority of the registered strong and weak vibrational bands of the fluoroform. This is due to using of the set of about 6÷8 sequentially increasing concentrations, at the time of monitoring of studied bands in the widest absorbance range of about 10^4. The spectroscopic measurements were carried out in such a way that the vibrational band, monitored at a known lower concentration and scaled by an adjusting factor, was fitted to the same bands recorded at a higher concentration quite well.

The Gaussian 98 program [29] was used to perform DFT and *ab initio* calculations. The optimized geometry, dissociation energy, dipole moment, frequency and infrared intensity of the normal vibrations of the molecules and complexes have been calculated at the DFT B3LYP and *ab initio* MO MP2 level of theory using the 6-311++G(3df,3pd) basis set. The interaction energy of the complex has been corrected for the basis set superposition error (BSSE), according to the Boys and Bernardi counterpoise method [30]. The features of the potential energy and dipole moment surfaces for CHF_3 and for F_3CH…B were analyzed using only B3LYP/6-311++G(3df,3pd) calculations.

RESULTS AND DISCUSSION

Results of measurements in the range of 1000–3100 cm^{-1}: Reviewed spectrum of fluoroform in Ar is shown in Fig. 1. The IR spectrum is characterized by closely located fundamental frequencies of the CF-stretching vibrations $\nu_2(A_1)$ and $\nu_5(E)$, which results in numerous resonance interactions of Darling – Dennison type in overtone region (for example the spectral region denoted by number 3) [31]. A strong Fermi resonance between the C–H stretching and bending modes of the molecule (peaks marked as 5 and 6) [32,33] also noticeably modifies the spectrum. The spectral parameters for some bands measured in the range of about 1000 up to 3100 cm^{-1} in liquefied Ar, N_2, CO and CO_2 are collected in Table 1. The parameters of the $\nu_4(E)$ band measured in CO_2 should be considered as only a crude estimation, due to overlapping with the intense induced bands (10^o0_2, 10^o0_1) of liquid carbon dioxide. The gas phase data [32–36] are also given for comparison. The most striking result is a strong decrease of the absolute intensity of $\nu_1(A_1)$ band in the studied series of solvents, with rather small variations of intensity of $\nu_2(A_1)$, $\nu_5(E)$ and $\nu_4(E)$ bands, being observed simultaneously. Moreover, frequency of ν_1 vibration exhibits a significant blue shift $\Delta\nu_1 = \nu_1^{sol} - \nu_1^{gas}$. The blue shift reaches +21.5 cm^{-1} in a liquid carbon dioxide as a solvent. It should be noted that the correction for the internal field effect does not exceed 1.10–1.15 in liquefied Ar, N_2, CO and CO_2 as a solvents. Being no larger than the inaccuracy of absolute intensity measurements, the effect cannot mask the observed trends. One could expect even further increasing of the effect of blue frequency shift and decreasing the intensity of the $\nu_1(A_1)$ band in the case of a specially selected partners. The substantial blue shift of the order of +19 cm^{-1} and the large decrease of the intensity value of 2.4 km/mol was reported for F_3CH…$O(CD_3)_2$ complex [37]. At the same time, a transition to a conventional red shift of the order of –21 cm^{-1} with integrated intensity value of about 6.2 km/mol has been noted in the same work for F_3CH…$N(CD_3)_3$ complex.

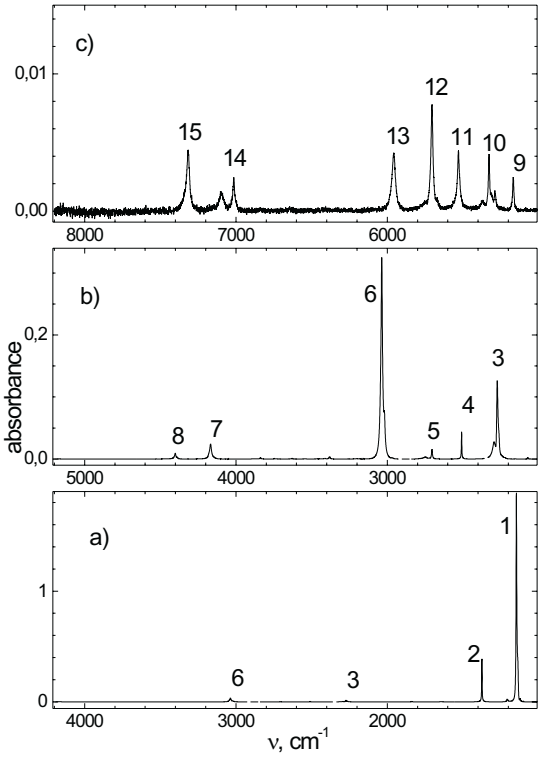

Figure 1. Reviewed spectrum of CF_3H in liquefied Ar. T~100 K, l =8.5 cm; $n(CF_3H)$ ~$5.8\cdot10^{16}$, $5.8\cdot10^{17}$, $5.8\cdot10^{18}$ molec/cm^3 for a), b), and c) respectively; 1 – $\nu_2(A_1)$, $\nu_5(E)$, $\nu_3 + \nu_6(E)$; 2 – $\nu_4(E)$; 3 – $2\nu_2(A_1)$, $\nu_2 + \nu_5(E)$, $2\nu_5(E)$; 4 – $\nu_2 + \nu_4(E)$, 5 – $2\nu_4(A_1, E)$; 6 – $\nu_4 + \nu_5 + \nu_6(A_1)$, $\nu_1(A_1)$; 7 – $\nu_1 + \nu_2(A_1)$, $\nu_1 + \nu_5(E)$; 8 – $\nu_1 + \nu_4(E)$; 9 – $\nu_1 + \nu_{2(5)} + 2\nu_6(E)$, $\nu_1 + 2\nu_{2(5)}(E)$; 10 – $4\nu_4(A_1)$; 11 – $\nu_1 + \nu_4 + \nu_5(E)$, $\nu_1 + \nu_2 + 2\nu_3(A_1)$; 12 – $\nu_1 + 2\nu_4(A_1)$; 13 – $2\nu_1(A_1)$; 14 – $\nu_1 + 3\nu_4(E)$, $2\nu_1 + \nu_2(A_1)$, $2\nu_1 + \nu_5(E)$; 15 – $2\nu_1 + \nu_4(A_1)$.

Fig. 2 displays the intensity decreasing and blue shift effects revealed for the ν_1 band of fluoroform in the studied series of solvents. The band is perturbed by a weak resonance interaction with $\nu_4 + \nu_5 + \nu_6(A_1)$ combination band with the interaction matrix element $W_{1456} = 3.68$ cm^{-1} [36], and by a stronger Fermi resonance $2\nu_4(A_1)$ with $W_{144} = 111.5$ cm^{-1} [33]. By modifying the spectral parameters of the ν_1 band, the mentioned resonance interactions do not change the direction of the effects observed. The unperturbed values of the frequency ν_1^0, absolute intensity I_1^0, frequency shift $\Delta\nu_1^0$ and the relative intensity $I_{rel}^0 \equiv I_{1(sol)}^0 / I_{1(gas)}^0$ are given in Table 2. They have been obtained by the standard formulae describing the vibration resonance interactions [31–33]:

$$\sqrt{R_0} = \sqrt{\frac{\kappa + \Delta}{\kappa - \Delta}} \cdot \frac{1 - \sqrt{R} \cdot \sqrt{\dfrac{\kappa - \Delta}{\kappa + \Delta}}}{1 + \sqrt{R} \cdot \sqrt{\dfrac{\kappa + \Delta}{\kappa - \Delta}}}, \qquad \text{where } \Delta = \sqrt{\kappa^2 - 4W^2}$$

where κ is an experimental splitting between Fermi doublet components, Δ – is the non-perturbed splitting between components of the doublet, R is the observed relative integrated intensity of the components, R_0 is the relative integrated intensity of the non-perturbed components. There were made attempts to treat the effect of decreasing intensity in terms of the Onsager reaction field model for the CHF_3/Ar and CHF_3/N_2 systems [24]. The desired decrease of the intensity was reproduced with an unrealistically small value of the spherical cavity radius $a_0 \sim 1.5$ Å only, instead of a more reasonable value of about 1.9–2.2 Å [6]. The frequency shift calculated in terms of the same model was found to be too small and practically independent of the solvent nature [38].

Table 1. Frequency – ν, full width at half maximum – 2Γ, and absolute integrated intensity – *I* of some IR bands of CF_3H in the region ~1000–3100 cm^{-1}.

	Assignment (Symmetry)	ν_2 (A_1)	ν_5 (E)	ν_4 (E)	$2\nu_4$ (A_1)	$2\nu_4$ (E)	$\nu_4+\nu_5+\nu_6$ (A_1)	ν_1 (A_1)
Gas phase [15–19]	ν, cm^{-1}	1141.5	1158.3	1377.9	2710.2	2754.8	3029	3035.2
	I, km/mol	129	525	88	1.0	0.16	–	24
Ar T ~100 K	ν, cm^{-1}	1137.3	1146.9	1374.5	2704.8	2748.4	3018.6	3036.7
	2Γ, cm^{-1}	7.6	4.9	3.4	6.9	24.5	9.3	11.7
	I, km/mol	80	440	60	0.48	0.34	1.9	18
N_2 100 K	ν, cm^{-1}	1140	1146.3	1376.5	2707.9	2754.2	3022.7	3047.4
	2Γ, cm^{-1}	9	6.5	4.8	8.8	35	24.8	14.9
	I, km/mol	88	480	56	0.24	0.44	1.2	15
CO 100 K	ν, cm^{-1}	1136	1142.0	1376.0	2706.4	3753.4	3018.0	3052.3
	2Γ, cm^{-1}	6.5	7	5.2	10.1	36	25	13.3
	I, km/mol	82	500	64	0.20	0.58	0.48	14
CO_2 230 K	ν, cm^{-1}	1132	1139.3	~1380	~10	~70	3027.3	3056.7
	2Γ, cm^{-1}	9.8	13.8	~10	26	61	51	27.5
	I, km/mol	106	560	~70	0.082	0.50	1.0	6.6

Results of the DFT and *ab initio* calculations: The present DFT B3LYP and HF/MP2 calculations predict minima only for the $F_3CH\ldots B$ (B = Ar, N_2, CO and CO_2) linear structures. The $F_3CH\ldots CO$ heterodimer is more stable than the $F_3CH\ldots OC$ structure. The linear geometry has also been found for the model of the $F_3CH\ldots NH_3$ heterodimer and for the $F_3CH\ldots N(CD_3)_3$ system characterized by noticeably stronger interactions. The calculated values of $r_e \equiv r_e$(C–H) and $R_e \equiv R_e$(C…B), the interaction energy D_e and the corrected energy D_e^{cor} for BSSE of the linear heterodimers are collected in Table 3. The calculated intensities and frequencies of the fundamental bands of fluoroform are also listed. Rather small variations of the positions and the absolute intensities of ν_2, ν_3, ν_4, ν_5 and ν_6 bands are predicted.

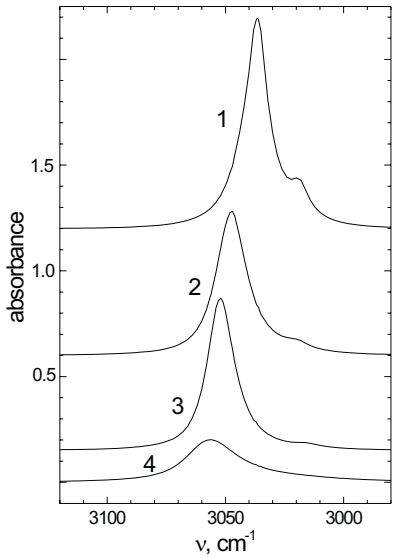

Figure 2. The $\nu_1(A_1)$ band of CF_3H dissolved in various cryogenic solutions. $n(CF_3H) = 1.5 \cdot 10^{19}$ molec/cm^3, $l = 1.0$ cm; 1 – Ar, $T \sim 100$ K; 2 – N_2, 100 K; 3 – CO, 100 K; 4 – CO_2, 230 K.

Table 2. Measured and predicted spectroscopic parameters for the ν_1 band of CHF_3/B systems. ν_1^0(cm^{-1}) – frequency and I_1^0(km/mol) – intensity corrected for Fermi resonances.

	ν_1^0	I_1^0	$\Delta\nu_1^0$			I_{rel}^0		
	Exp.	Exp.	Exp.	B3LYP	MP2	Exp.	B3LYP	MP2
Gas	3017.3	25.6	–	–	–	1.0	1.0	1.0
Ar	3020.1	20.2	+2.8	+2.0	+12	0.79	0.87	0.63
N_2	3031.4	16.2	+14.1	+17	+30	0.63	0.39	0.20
OC				+16	+26		0.47	0.36
CO	3036.4	14.6	+19.1	+16	+26	0.57	0.20	0.12
CO_2	3040.9	7.6	+23.6	+27	+37	0.30	0.21	0.11
$(CD_3)_2O$	3036*)	2.5*)	+18.7*)	?	–	0.1*)	?	–
NH_3	–	–	–	–13	–	–	0.7	–
$(CD_3)_3N$	2995*)	7*)	–22.3*)	–58**)	–	0.27*)	1.8**)	–

Note: *) – data obtained in liquid Ar at T ~ 92 K [37], **) – preliminary results.

On the contrary, the ν_1 band is characterized by a noticeable blue shift of frequency and a strong decrease of the intensity. All these predictions are in accordance with the trends observed experimentally. They are presented in Table 2 (see also Table 1). MP2 calculations predict noticeably stronger effects, however, the less time consuming DFT method results are closer to the experimental data. Note that the data computed for $B = NH_3$, $N(CD_3)_3$ and experimentally obtained for $B = N(CD_3)_3$ [37] are characterized by the usual low frequency shift of ν_1. DFT and *ab initio* calculations show analogous unusual tendency of increasing the contraction of r_e distance, when going

from Ar to CO_2. In the case of the substantially stronger system, like $F_3CH\ldots NH_3$, the value of r_e increases (Table 3). Previous computation results, obtained for the $F_3CH\ldots N(CD_3)_3$ system, suggest even a larger growth of CH bond length (r_e ~1.0928 Å), with the decrease of the distance between C and N atoms ($R_e(C\ldots B)$ ~3.372 Å) simultaneously. Moreover, the calculations predict the substantial red frequency shift and noticeable intensity growth of the CH band in the case of the $F_3CH\ldots N(CD_3)_3$ heterodimer, which are typical for conventional H-bonds. The predictions qualitatively correspond to experimentally observed effects. Preliminary estimations in the framework of the performed calculations with a modest basis set show a blue frequency shift with a remarkable decreasing intensity for the linear $F_3CH\ldots O(CD_3)_2$ complex.

Table 3. Predicted structural and spectroscopic parameters of $F_3CH...B$ linear complexes.

B		Free F1	Ar	N_2	OC	CO	CO_2	NH_3
r_e(CH), Å	B3LYP	1.089	1.0889	1.0882	1.0882	1.0882	1.0877	1.0897
	MP2	1.0845	1.0841	1.0835	1.0837	1.0835	1.0832	–
R_e(C...B), Å	B3LYP	–	4.390	3.818	3.744	3.846	3.573	3.444
	MP2	–	3.931	3.599	3.576	3.703	3.436	–
D_e, kJ/mol D_e^{cor}, kJ/mol	B3LYP	–	0.33 0	2.4 1.5	2.1 1.3	3.9 2.9	4.5 3.5	16 15
	MP2	–	2.9 2.3	6.4 4.8	4.6 3.3	8.1 6.7	8.1 6.7	–
ν_1, cm^{-1} I_1, km/mol	B3LYP	3126.6 28	3128.6 24	3143.6 11	3143.0 13	3142 5.4	3153.8 5.8	3113.8 19
	MP2	3200 24	3213 15	3231 4.8	3226 8.8	3227 2.8	3237 2.6	–
ν_2, cm^{-1} I_2, km/mol	B3LYP	1133 94	1133 110	1131 120	1131 120	1130 120	1130 130	1118 137
	MP2	1165 95	1164 114	1162 120	1163 120	1161 120	1162 138	–
ν_3, cm^{-1} I_3, km/mol	B3LYP	693 12	693 14	693 15	693 16	692 16	692 17	688 19
	MP2	712 13	712 15	711 16	711 16	710 17	711 18	–
ν_4, cm^{-1} I_4, km/mol	B3LYP	1381 72	1384 75	1392 72	1389 72	1394 73	1394 70	1426 58
	MP2	1420 86	1426 90	1438 82	1433 84	1438 84	1438 80	–
ν_5, cm^{-1} I_5, km/mol	B3LYP	1131 610	1132 600	1129 600	1130 600	1127 600	1127 600	1114 606
	MP2	1187 600	1186 570	1184 580	1186 580	1182 580	1183 580	–
ν_6, cm^{-1} I_6, km/mol	B3LYP	500 3.6	500 3.4	500 3.4	500 3.4	500 3.2	500 3.2	500 3.5
	MP2	516 4.6	516 4.6	516 4.2	516 4.2	515 4.2	516 4.2	–

Fig. 3 presents typical examples of dipole moment functions μ(r) predicted by the DFT/B3LYP calculations. Note that the calculations have been performed at a fixed center of mass position of the systems studied, by taking into the account small displacements of the C atom characterized by a relatively large charge. The dipole moment μ decreases with elongation of the CH bond for free fluoroform. This is due to opposite directions of the dipole moment of CH bond and the dipole moment of the whole molecule [23,25,39]. A noticeable flattening of the μ(r) is observed, when going to the $F_3CH\ldots CO$ system. Nevertheless, the dipole moment μ(r) still remains a decreasing function of r(CH). In the case of the $F_3CH\ldots NH_3$ complex, the dipole moment begins to increase on the elongation of CH bond. Fig. 4 displays the predicted trends for the bond length variation Δr_e, frequency shift $\Delta\nu_1$ and the first derivative μ of the dipole moment with respect to dimensionless normal coordinate Q_1 as a function of D_e^{cor}. The z axis is directed along the C_∞ axis of the linear $F_3CH\ldots B$ structure. All the functions are polynomial fits constructed on the basis of data calculated for B = Ar, N_2, CO, CO_2 and NH_3. In fact, the μ′ value practically determines the ν_1 band intensity. It should be noted that μ′ is negative for weaker complexes, it passes through the zero and then becomes positive, appreciably growing in the case of stronger complexes. Thus, a decrease of the intensity, accompanied by a noticeable high frequency shift of ν_1 band, and then the transition to a red shift with increasing intensity of the band, is predicted for the systems studied. The last result is in accordance with that observed experimentally for a stronger $F_3CH\ldots N(CD_3)_3$ complex [23,25,37]. Somewhat weaker $F_3CH\ldots O(CD_3)_2$ complex exhibits a maximum decrease of inten-

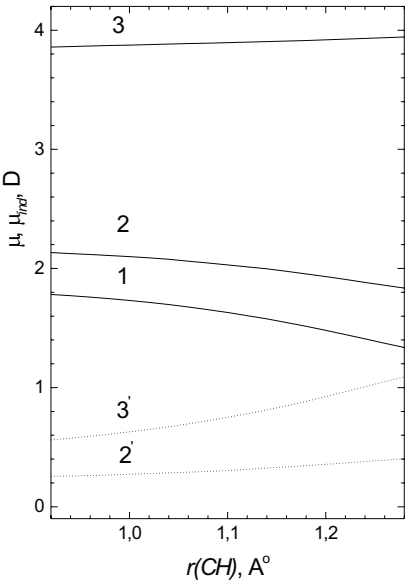

Figure 3. μ (solid line) and μ_{ind} (dotted line) functions with respect to *r*(C–H). 1 – free CF_3H, 2, 2′ – $F_3CH\ldots CO$, 3, 3′ – $F_3CH\ldots NH_3$.

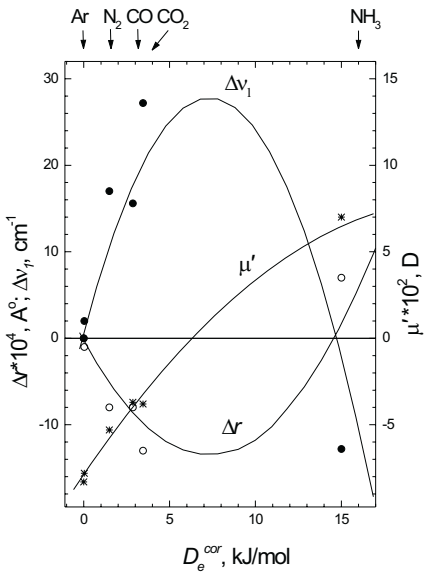

Figure 4. Predicted Δr_e(C–H), $\Delta\nu_1$ and μ' functions *versus* to D_e^{cor}. Open circles, solid circles and stars are computed data for Δr_e(C–H), $\Delta\nu_1$ and μ' respectively; solid lines are polynomial fits for the computed data.

sity observed experimentally, down to about 2.5 km/mol. The predicted behavior is naturally explained by an increase of the dipole moment of the complex (μ), due to an induced moment (μ_{ind}) contribution: $\mu = \mu_{Fl} + \mu_B + \mu_{ind}$ [4,40], where μ_{Fl} is a dipole moment of fluoroform molecule. The dipole moment of fluoroform molecule is characterized by the described non-typical behavior, whereas μ_{ind} exhibits the ordinary variation, namely it increases with elongation of r (see curves 2′, 3′ in Fig. 3). Note that μ_{ind} noticeably grows during passing to stronger complexes. As a result of such a competition, the sign of the first derivative of μ^z with respect to Q_1 is changed from negative to positive and the increase following decrease of absolute value. As a result, there is no fundamental difference between the interactions in the $F_3CH\ldots B$ complex and those accepted as a conventional hydrogen bond. In fact, any molecule, characterized by a negative value of the first derivative of the dipole moment (or by the dipole moment function with its maximum value occurring near the equilibrium position), might show an effect of decreasing (or non-monotonously varying) intensity of a stretching band due to a proper intermolecular interaction.

The blue shift effect on ν_1 frequency of $F_3CH\ldots B$ is naturally obtained in the terms of second order perturbation theory, taking the potential of intermolecular interaction $U(Q_1) \equiv E_c(Q_1) - E_m(Q_1)$ and the cubic term $\alpha_{111}Q_1^3$ as a perturbation [6]:

$$\Delta\nu_1 \approx \frac{1}{2}\frac{\partial^2 U}{\partial Q_1^2} - \frac{3\alpha_{111}}{\omega_1}\frac{\partial U}{\partial Q_1} + \ldots$$

where E_c is the energy of the $F_3CH\ldots B$ complex, E_m is the energy of free F_3CH, $\alpha_{111} \sim -320$ cm^{-1} [41]. Fig. 5 shows an example of computed U, U′ and U″ functions, which are typical of the systems characterized by a blue frequency shift. The change of the potential of intermolecular interaction $U(Q_1)$ from the repulsive-type (U′, U″ > 0) for $F_3CH\ldots B$ (B = Ar, N_2, CO, and CO_2) to a domination of attractive type of interaction (U′, U″ < 0) in the case of $F_3CH\ldots NH_3$ has been predicted by the present calculations. This results in transition from a blue frequency shift to a red shift. The latter effect correlates with transition from a contraction to a conventional elongation of the CH bond (see Fig. 4), while going to the stronger bond complexes.

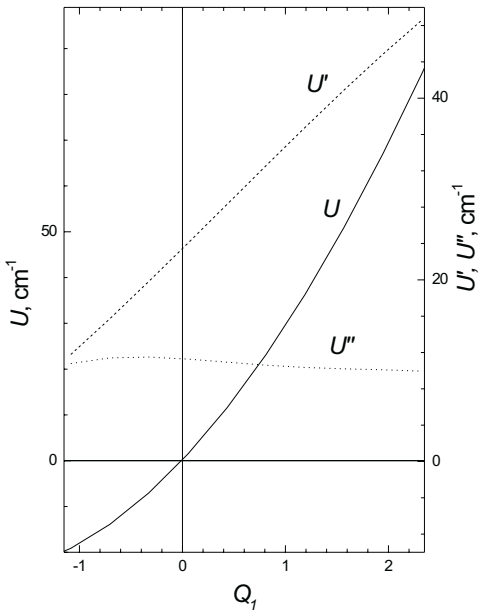

Figure 5. The intermolecular potential $U(Q_1)$, its first $U'(Q_1)$ and second $U''(Q_1)$ derivatives with respect to dimensionless normal coordinate Q_1, calculated for $F_3CH\ldots CO$ system.

Results of measurements in the range of the overtone and combination transitions: Table 4 collects spectral parameters for some overtone and higher order combination bands of fluoroform measured in the range of about 4000–9000 cm^{-1}. A considerable blue shift is also noted in the case of most combination and overtone bands with ν_1 vibration being excited. However, the variation of the intensity is not so noticeable and regular as for ν_1 band. For example, the first overtone $2\nu_1$ is blue shifted by +21.6 cm^{-1}, +29.6 cm^{-1} and +34.4 cm^{-1} in N_2, CO and CO_2 respectively, whereas the absolute intensity of this band is somewhat larger in these solvents than that measured in the gas phase. The non-typical weak increase (instead of a conventional noticeable decrease) of intensity of the first overtone $2\nu_1(A_1)$, observed in $F_3CH\ldots B$ (B = N_2, CO, CO_2), can be explained also by the features of the dipole mo-

ment function found in the present theoretical calculations. The transition moment of the first overtone, derived in the framework of second-order perturbation theory, is:

$$< 0| \mu^z| 2 > \approx \frac{1}{2\sqrt{2}} \frac{\partial^2 \mu^z}{\partial Q_1^2} + \frac{\alpha_{111}}{\sqrt{2} \cdot \omega_1} \frac{\partial \mu^z}{\partial Q_1} + \ldots \quad (1)$$

The calculations predict the same signs of the first and second derivatives of μ^z for the systems studied. They are negative for the free CHF_3 and for $F_3CH\ldots B$ (B = N_2, CO, and CO_2), while become positive in the case of a noticeably stronger $F_3CH\ldots NH_3$ complex. Thus, the mutual compensation of the terms in (1) ($\alpha_{111} < 0$) favors a weak variation of the absolute intensity of $2\nu_1$ in the series studied. As a result, a weak growth of intensity could be expected in the case of a decrease of absolute value of the first derivative of the μ^z.

Table 4. Spectroscopic parameters of some overtone and higher order combination bands of CF_3H in the region ~4000–9000 cm^{-1}.

	Assign. (Symmetry)	$\nu_1 + \nu_4$ (E)	$4\nu_4$ (A_1)	$\nu_1 + 2\nu_4$ (A_1)	$2\nu_1$ (A_1)	$\nu_1 + 3\nu_4$ (A_1)	$2\nu_1 + \nu_4$ (E)	$2\nu_1 + 2\nu_4$ (A_1)	$3\nu_1$ (A_1)
Gas phase [15–19]	ν, cm^{-1}	4400	5337	5710.4	5959.2	7018	7322	8589.3	8792.7
	I, km/mol	–	–	0.034	0.052	–	–	–	–
Ar T~100 K	ν, cm^{-1}	4401.6	5328.1	5704.9	5957.9	7014.3	7317.2	8581	–
	2Γ, cm^{-1}	11.3	9.7	16.2	26	16.6	25	31	–
	I, km/mol	0.44	0.016	0.068	0.048	0.016	0.048	0.014	–
N_2 ~100 K	ν, cm^{-1}	4413.4	5335.2	5719.5	5980.8	7030	7340.9	8609	–
	2Γ, cm^{-1}	14.3	14.1	20.9	36	21.9	36.5	40	–
	I, km/mol	0.58	0.016	0.056	0.060	0.016	0.052	0.012	–
CO ~100 K	ν, cm^{-1}	4416.0	5332.9	5722.0	5988.8	7033.6	7349.5	–	–
	2Γ, cm^{-1}	14.9	19.8	20	36	24	39	–	–
	I, km/mol	0.96	0.026	0.070	0.074	0.022	0.078	–	–
CO_2 ~230 K	ν, cm^{-1}	4420.6	5328.0	5724.4	5993.6	7036.1	7355.3	8618.9	8840.4
	2Γ, cm^{-1}	27	38	42	66	38	67	109	126
	I, km/mol	0.82	0.022	0.060	0.062	0.012	0.062	0.014	0.008

The region of the $2\nu_1(A_1) \approx \nu_1 + 2\nu_4(A_1) \approx 4\nu_4(A_1)$ Fermi resonance polyad [31–33], with several new combination bands in the spectrum of the systems studied, is shown in Fig. 6. In addition to the polyad, there are two bands of comparable intensity and five bands of markedly weaker intensity. In the case of CO_2 as a solvent, the last bands are masked by wings of stronger $\nu_1 + 2\nu_4$ and $4\nu_4$ bands, due to temperature broadening effects. The two bands of comparable intensity can be ascribed to $\nu_1 + \nu_3 + \nu_4(E)$ and $\nu_1 + \nu_4 + \nu_5(E)$ modes respectively. The reliable assignment of the last five weak bands of fluoroform needs a separate study. In CO and CO_2 as solvents, new ν_x

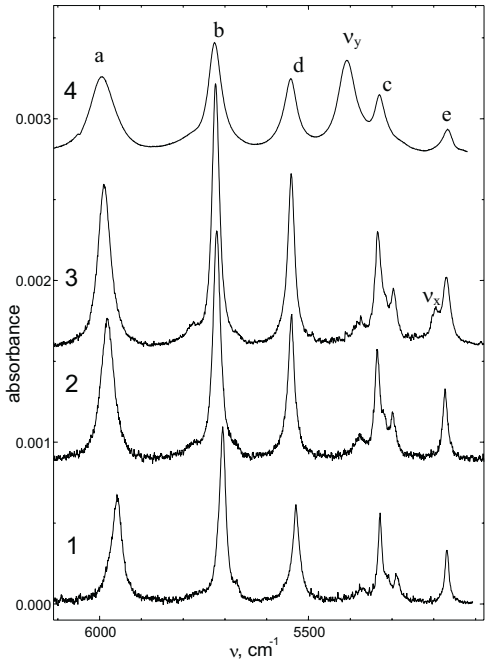

Figure 6. The $2\nu_1(A_1)\div4\nu_4(A_1)$ region in the IR spectrum of CF_3H dissolved in various cryogenic solutions. $n(CF_3H) = 9\cdot10^{18}$ molec/cm^3, $l = 1.0$ cm; 1 – Ar, T ~ 100 K; 2 – N_2, 100 K; 3 – CO, 100 K; 4 – CO_2, 230 K; a – $2\nu_1(A_1)$, b – $\nu_1 + 2\nu_4(A_1)$, c – $4\nu_4(A_1)$, d – $\nu_1 + \nu_3 + \nu_4(E)$, e – $\nu_1 + \nu_4 + \nu_5(E)$, $\nu_x = \nu_1(CF_3H) + \nu(CO)$; $\nu_y = \nu_1(CF_3H) + \nu_3(CO_2)$.

and ν_y bands have been detected. The frequencies of these bands are close to the $\nu_1 + \nu_{CO}$ and $\nu_1 + \nu_{3,CO_2}$ frequencies, respectively. The absolute intensity of the latter band exceeds the intensity of the former band by about 7. Another additional band, whose frequency is close to $\nu_2 + \nu_{CO}$ and $\nu_5 + \nu_{CO}$ positions, was revealed in CO as a solvent. In fact, all the last three combination bands correspond to the simultaneous transitions of the type: $\nu_i(A) + \nu_j(B)$. Here, $A \equiv CHF_3$, $B \equiv N_2$, CO, CO_2. Spectroscopic parameters of these bands are given in Table 5. In the case of a dipole induction approximation of an effective field, produced by a system of point charges of A(B) in B(A), one obtains a simple relation for the transition dipole moment of $\nu_1(CHF_3) + \nu_j(B)$:

$$< 1,1|\ \mu^z|\ 0,0 > \approx \frac{1}{R^3}\left(\frac{\partial \alpha_{Fl}^{zz}}{\partial Q_1} \cdot \frac{\partial \mu_B^z}{\partial Q_j} + \frac{\partial \mu_{Fl}^z}{\partial Q_1} \cdot \frac{\partial \alpha_B^{zz}}{\partial Q_j} \right)$$

Here, $Q_j = Q_{N_2}$, Q_{CO} or Q_3 of CO_2; R is the distance between the interaction centers, which can be considered as an adjusting parameter in crude estimations. If one locates the center of oscillating dipole of the CH stretch vibration near the H atom, the R – effective distance for the systems studied are 3.3 Å, 3.35 Å and 3.67 Å for $F_3CH\ldots N_2$, $F_3CH\ldots CO$, and $F_3CH\ldots CO_2$ respectively, and the corresponding intensities of the

simultaneous transitions are $2\cdot10^{-4}$ km/mol, $2\cdot10^{-2}$ km/mol and $6\cdot10^{-2}$ km/mol. The estimations have been performed using literature values of electric parameters: $(\partial\alpha_{Fl}^{zz})/(\partial Q_1) = 0.234$ Å^3 [42] and $(\partial\mu_{Fl}^{z})/(\partial Q_1) = -0.08$D [33] for CHF_3; $(\partial\alpha_{B}^{zz})/(\partial Q_j) = 0.056$ Å^3 [43] for N_2; $(\partial\alpha_{B}^{zz})/(\partial Q_j) = 0.144$ Å^3 [43] and $(\partial\mu_{B}^{z})/(\partial Q_j) = -0.15$D [43] for CO; $(\partial\mu_{B}^{z})/(\partial Q_j) = 0.45$D [44] for ν_3 of CO_2. The estimated values of intensities truly reflect the experimental finding, namely lack of the combination band in the case of N_2 and the strongest simultaneous transition in the case of CO_2. The data obtained suggest a major contribution of electrostatic forces into weakly bond interactions for the systems studied. Nevertheless, a careful evaluation of the strength of these combination bands can be performed if the dipole moment function of the relevant normal coordinates and anharmonic terms of PES of interacting pairs would be found.

Table 5. Spectroscopic parameters of the combination bands with simultaneous vibrational excitation of CF_3H and *B* (*B* = CO, CO_2) partners. Units of the parameters are the same as in Table 1.

$\nu(CHF_3) + \nu(B)$	ν	2Γ	*I*
$\nu_{2(5)} + \nu(CO)$	3280.3	12.3	0.016
$\nu_1 + \nu(CO)$	5197.0	24	0.008
$\nu_1 + \nu(CO_2)$	5407.7	50	0.056

The full width at half maximum 2Γ reveals a remarkable variation in the set of the bands recorded. In the case of the perpendicular bands, corresponding to an E – symmetry vibrations (*e.g.* ν_4(E) and $2\nu_4$(E)), the observed variation could be treated in the framework of first order Coriolis coupling [45,46]. Thus, the parallel bands, which are non-disturbed by the Coriolis interaction, should be characterized by weaker variations of the width, if hindering of rotational motion would be the main band shaping mechanism. Nevertheless, the ν_1 band has a markedly larger 2Γ than other first and some higher order parallel bands (see Table 1 and Table 4). Moreover, the width of the first overtone $2\nu_1$ increases by a factor of ≥2. The results obtained in CO_2 suggest a further broadening by a factor of ≥2, when going to the second overtone $3\nu_1$. A preliminary band shape analysis have shown, that the ν_1 band is characterized by a Voigt-like profile, with the width of Lorentz $2\Gamma_L$ and Gauss $2\Gamma_G$ parts, which are comparable. For example, $2\Gamma_L = 11.4$ cm^{-1}, $2\Gamma_G = 7.9$ cm^{-1} in liquid N_2 (T ~ 100 K). The observed broadening and band shape effects suggest the substantial role of inhomogeneous vibrational relaxation in the case of ν_1 mode [47]. Analogous broadening effects are also manifested for ν(A–H) mode of the hydrogen-bonded AH…B systems, due to low frequency modes contributing to hot transitions [48]. For all the registered bands, 2Γ tends to grow in the studied series of solvents. A noticeable temperature effect on the width of bands cannot be excluded for CO_2 as a solvent.

CONCLUSIONS

The blue frequency shift accompanied by a decreasing intensity of the C–H stretching band of CF_3H have been found to increase in the series of liquefied Ar, N_2,

CO and CO_2 solutions. Results of the DFT and *ab initio* calculations predict a weak complex formation, with the increase of the equilibrium dissociation energy of the $F_3CH\ldots B$ linear structure in the series studied Ar, N_2, CO, and CO_2. They reproduce unusual trends observed in the bulk experiments. The spectroscopic features of the fluoroform, dissolved in liquefied Ar, N_2, CO and CO_2, have been explained by a non-typical increase of the dipole moment with contraction of the C–H bond of free CF_3H, accompanied by a conventionally varying induced dipole moment. A transition to a red frequency shift and increasing intensity of the C–H stretch band, which is typical of conventional H-bonded systems, has been predicted in the case of stronger $F_3CH\ldots B$ complexes, characterized by a larger value of induced dipole moment. In the case of $2\nu_1$ and some combination bands, a blue shift and a weak growth of the intensity were observed. Weak combination bands, attributed to the simultaneous vibrational excitation of the interacting pairs, have been revealed in CF_3H/CO and $/CO_2$ systems. Obtained results suggest a major contribution of electrostatic interactions in the systems studied.

Acknowledgments

This work was financially supported by the Polish State Committee for Scientific Research (Grant No 7T09A 008/21). S.M.M. and K.S.R. thank for support RFBR-DFG, (Grant No. 99-03-04026). The authors gratefully acknowledge Professor E.S. Kryachko for fruitful discussions. The Wrocław Supercomputer Center and Academic Computer Center CYFRONET-CRACOW (supported by KBN – research project no. KBN/SGI_ORIGIN_2000/UWrocł./067/2000), where some of the calculations have been performed, are gratefully acknowledged for providing the computer time and facilities.

REFERENCES

1. Pimentel G.C. and McClellan A.L., *Ann. Rev. Phys. Chem*., **22**, 347 (1971).
2. Scheiner S., Hydrogen Bonding, Oxford University Press, NY 1997, p. 359.
3. Iogansen A.V., in: N.D. Sokolov (Ed.), Hydrogen Bond, Moscow, 1981, p. 112.
4. Tchulanowsky V.M. and Khaikin S.Ya., *Opt. Spectrosc*., **23**, 709 (1967) (in Russian).
5. Sandorfy C., The Hydrogen Bond – Recent Developments in Theory and Experiments (Eds. P. Schuster *et al*.), North-Holland Publ. Co., Amsterdam, 1976, p. 615.
6. Buckingham A.D., *Proc. Roy. Soc*., **255**, 32 (1960).
7. Akiyama M., *J. Chem. Phys*., **84**, 631 (1986).
8. Onsager L., *J. Am. Chem. Soc*., **58**, 1486 (1936).
9. Terentjev V.A, Thermodynamics of Hydrogen Bonding (in Russian), Saratov University Press, Kujbyshev, 1973.
10. Gu Y., Kar T. and Scheiner S., *J. Mol. Struct*., **532**, 17 (2000).
11. Hartmann M. and Radom L., *J. Phys. Chem*., **A104**, 968 (2000).
12. Salvador P., Simon S., Duran M. and Dannenberg J.J., *J. Chem. Phys*., **113**, 5666 (2000).
13. Tokchadze K.G. and Tkhorzevskaya N.A., *J. Mol. Liq*., **32**, 11 (1986).
14. Antonenko G.V., Kolomiytsova T.D., Kondaurov V.A. and Snchepkin D.N., *J. Mol. Struct*., **275**, 183 (1992).
15. Jemmis E.D., Subramanian G., Nowek A., Gora R.W., Sullivan R.H. and Leszczynski J., *J. Mol. Struct*., **556**, 315 (2000).
16. Novoa J.J. and Mota F., *Chem. Phys. Lett*., **318**, 345 (2000).
17. Lee M., Jang H. and Ault B.S., *J. Phys. Chem*., **94**, 4851 (1990).
18. Hobza P. and Havlas Z., *Chem. Phys. Lett*., **303**, 447 (1999).
19. Cubero E., Orozco M. and Lique F.J., *Chem. Phys. Lett*., **310**, 445 (1999).

20. Hobza P., Spirko V., Havlas Z., Buchhold K., Reimann B., Barth H.D. and Brutschy B., *Chem. Phys. Lett*., **299**, 180 (1999).
21. Kryachko E.S. and Zeegers-Huyskens T., *J. Phys. Chem*., **105**, 7118 (2001).
22. Hobza P. and Havlas Z., *Chem. Rev*., **100**, 4253 (2000).
23. Golubev N.S., Kolomiitsova T.D., Melikova S.M. and Shchepkin D.N., in: Teoreticheskaya Spektroskopiya, Izv. Akad. Nauk SSSR (in Russian), 1977, p. 78.
24. Bulanin M.O., Kolomiitsova T.D., Kondaurov V.A. and Melikova S.M., *Opt. Spectrosc*., **68**, 763 (1990), (in Russian).
25. Bertcev V.V., Golubev N.S. and Shchepkin D.N., *Opt. Spectrosc*., **40**, 951 (1977) (in Russian).
26. Budesinsky M., Fiedler P. and Arnold Z., *Synthesis*, 858 (1989).
27. Boldeskul I.E., Tsymbal I.F., Ryltsev E.V., Latajka Z. and Barnes A.J., *J. Mol. Struct*., **436**, 167 (1997).
28. Rutkowski K.S., Melikova S.M., Shchepkin D.N., Lipkowski P. and Koll A., *Chem. Phys. Lett*., **325**, 425 (2000).
29. Frisch M.J. *et al*., Gaussian 98, Revision A.9, Gaussian, Inc., Pittsburgh PA, 1998.
30. Boys S.F. and Bernardy F., *Mol. Phys*., **19**, 553 (1970).
31. Kolomijtsova T.D., Melikova S.M. and Shchepkin D.N., *Opt. Spectrosc*., **67**, 592 (1989) (in Russian).
32. Segall J., Zare R.N., Dubal H.R., Lewerenz M. and Quack M., *J. Chem. Phys*., **86**, 634 (1987).
33. Dubal H.R., Ha T.K., Lewerenz M. and Quack M., *J. Chem. Phys*., **91**, 6698 (1989).
34. Sofue S., Kawaguchi K., Hirota E. and Fujiama T., *Bull. Chem. Soc. Jpn.*, **54**, 897 (1981).
35. Kondo S. and Saeki S., *J. Chem. Phys*., **74**, 6603 (1981).
36. Pine A.S., Fraser G.T. and Pliva J.M., *J. Chem. Phys*., **89**, 2720 (1988).
37. Antonenko G.V., Dissertation, Leningrad State University, Leningrad, 1989, pp. 1–172 (in Russian).
38. Cedeno D., Peng J., Reynolds D., Mina-Camilde N. and Manzanares C., *Mol. Phys*., **96**, 1745 (1999).
39. Masunov A., Dannenberg J.J. and Contreras R.H., *J. Phys. Chem*., **A105**, 4737 (2001).
40. Shchepkin D.N. and Melikova S.M., *J. Chim. Phys*., **89**, 607 (1992).
41. Klatt G., Willetts A., Handy N.C., Tarroni R. and Palmieri P., *J. Mol. Spectrosc*., **64**, 176 (1996).
42. Schretter H.W. and Kloekner H.W., in "Raman Spectroscopy of Gases and Liquids" (Ed. A.Weber), Springer Verlag, Berlin, 1979.
43. Bulanin M.O., Bulychev V.P. and Tokchadze K.G., *Opt. Spectrosc*., **67**, 579 (1989) (in Russian).
44. Rothman L.S. and Young L.D.G., *J. Quant. Spectrosc. Rad. Transf*., **25**, 505 (1981).
45. Kondaurov V.A., Melikova S.M. and Shchepkin D.N., *Opt. Spectrosc*., **56**, 1020 (1984) (in Russian).
46. Rutkowski K.S., Melikova S.M. and Shchepkin D.N., *Vibr. Spectrosc*., **24**, 227 (2000).
47. Gayathri N., Bhattcharyya S. and Bagchi B., *J. Chem. Phys*., **107**, 10381 (1997).
48. Shchepkin D.N., *J. Mol. Struct*., **156**, 303 (1987).